

The growth of various buffer layer structures and their influence on the quality of (CdHg)Te epilayers

G.J. Gouws, R.J. Muller and R.S. Bowden

Mikomtek CSIR, P.O. Box 395, Pretoria 0001, South Africa

Received 3 April 1992; manuscript received in final form 22 December 1992

The suitability of various buffer layer structures on (100) GaAs for (CdHg)Te growth by organometallic vapour phase epitaxy (OMVPE) was investigated. The preferred epitaxial orientation of (100)GaAs/(111)CdTe was found to be unsuitable due to the formation of electrically active defects in the material. An intermediate ZnTe layer was used to select the (100) orientation and (100) CdTe layers were then deposited on this ZnTe layer. The quality of the resultant CdTe buffer was found to critically depend on the thickness of this intermediate ZnTe buffer, with a ZnTe thickness of approximately 500 Å producing the best CdTe buffer. (CdHg)Te epilayers grown on these ZnTe/CdTe buffers had improved electrical properties, but still suffered from a poor surface morphology. This surface morphology could be improved by using a lattice matched Cd_{0.96}Zn_{0.04}Te alloy as the final buffer layer, but the surface pyramids typical of the (100) orientation could never be completely eliminated.

1. Introduction

CdTe would be the first choice as a substrate for (HgCd)Te epitaxy, as it has a small mismatch with Cd_{0.2}Hg_{0.8}Te and it is physically and optically very compatible. However, CdTe has the disadvantage that these substrates are often of relatively poor crystalline quality, not available in large areas and expensive. This has stimulated a search for an alternate hybrid substrate [1]. GaAs has become the most popular substrate material and device quality (CdHg)Te epilayers have been grown on these substrates [2,3]. However, the growth of a suitable buffer layer between the GaAs substrate and the (CdHg)Te epilayer is essential in order to take up the large lattice mismatch between the epilayer and substrate as well as to prevent the diffusion of any unwanted impurities from the substrate to the epilayer. Such a buffer should conform to the following requirements:

(i) It should be a good quality single crystal of the desired orientation.
(ii) It should prevent any impurities from diffusing from the substrate into the epilayer.

(iii) It should have a high electrical resistivity (semi-insulating) so as not to influence the conduction in the epilayer.

(iv) It should have a very smooth surface morphology.

(v) It should have a good lattice match with the epilayer to prevent the introduction of misfit dislocations into the epilayer.

The most commonly used substrate/buffer layer combination is a semi-insulating GaAs substrate of the (100) orientation together with a CdTe buffer layer of approximately 3 μm thick. This buffer is found adequate to accommodate the lattice mismatch and prevent Ga diffusion from the substrate.

This study will now attempt to evaluate the suitability of different buffer layers for (CdHg)Te epitaxy on (100) GaAs by OMVPE. The following buffer layer structures, schematically illustrated in fig. 1, were used:

- (a) Buffer A: CdTe of (111) orientation
- (b) Buffer B: ZnTe/CdTe combinations of (100) orientation
- (c) Buffer C: ZnTe to CdTe graded layers of (100) orientation

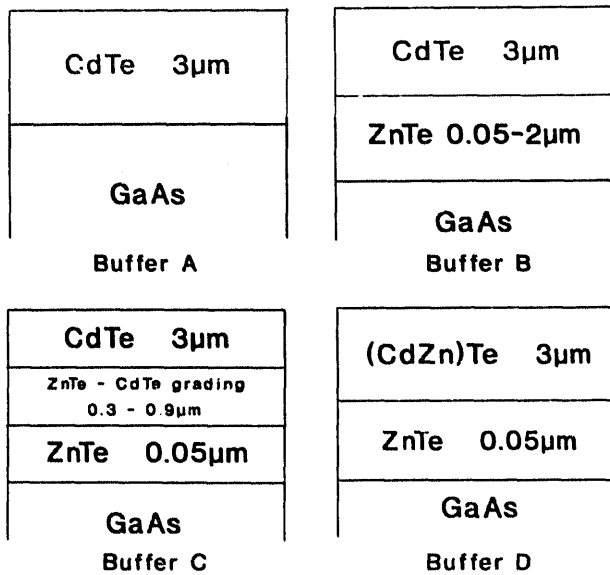


Fig. 1. The structure of the different buffer layers used in this study.

Table 1

Lattice parameters of various materials and the mismatch relative to that of $\text{Cd}_{0.2}\text{Hg}_{0.8}\text{Te}$

Material	Lattice parameter (Å)	Mismatch (%)
GaAs	5.653	14.3
CdTe	6.481	0.3
ZnTe	6.104	5.9
$\text{Cd}_{0.2}\text{Hg}_{0.8}\text{Te}$	6.464	-
$\text{Cd}_{0.2}\text{Zn}_{0.04}\text{Te}$	6.467	0

(d) Buffer D: lattice matched $\text{Cd}_{0.96}\text{Zn}_{0.04}\text{Te}$ alloys of (100) orientation.

In table 1 the lattice parameters of the materials used in this work are compared to that of $\text{Cd}_{0.2}\text{Hg}_{0.8}\text{Te}$.

2. Experimental procedure

All the layers were grown in an MR Semicon Quantax 226 OMVPE reactor, using DIPTe , DMCd and DEZn as the precursors for the buffer layers, while liquid Hg was added for the growth of $(\text{CdHg})\text{Te}$. Palladium-purified H_2 was used as the carrier gas. The substrate orientations were both (100) and 2° off (100) from various vendors.

No significant differences were found in the results on these different substrates. The GaAs substrate was always first treated to a pregrowth bake at 620°C under H_2 flow for 15 min to clean the surface of adsorbed oxides, after which buffer growth was performed at a temperature of 365°C . The $(\text{CdHg})\text{Te}$ layers were grown at the same temperature.

The cell design incorporates an integral upstream bath for liquid Hg, with separate flows of H_2 over the Hg and supplying the organometallics. During the buffer layer growth this bath was empty, but a low flow of H_2 was passed through the bath to prevent the recirculation of reactants from the main part of the cell.

A gas flow velocity of 10.5 cm/s was used during the growth of the buffer layers and the CdTe cycle of the IMP process. For the HgTe cycle of the IMP, a flowrate of 3.8 cm/s was used. The Te mole fraction was kept at 3×10^{-4} during buffer growth and the CdTe cycle and at 8.4×10^{-4} during the HgTe cycle. A II/VI ratio of 1 was used for both ZnTe and CdTe growth, the Hg bath was kept at a temperature of 220°C for the CMT growth.

After the buffer layers were removed from the reactor, a piece was cleaved off for characterization and the remaining piece stored in atmosphere for later $(\text{CdHg})\text{Te}$ growth. The buffers were not given any chemical cleaning before $(\text{CdHg})\text{Te}$ growth, but the surface dust was removed by blowing with high purity nitrogen gas. The buffer layer was then given a pregrowth bake at 500°C for 5 min to desorb the surface oxides. In some cases the buffer layer was also chemically degreased before it was loaded, but this step showed no advantage over the normally prepared layers and this procedure was not adopted.

Pieces of approximately 1 cm^2 of the various buffer layer structures were then placed simultaneously in the reactor and a $12 \mu\text{m}$ thick layer of $\text{Cd}_{0.22}\text{Hg}_{0.78}\text{Te}$ was grown by the IMP process [4]. A CdTe cap of approximately $0.1 \mu\text{m}$ was grown as a last step to preserve the surface of the layer during the subsequent in situ anneal and cooldown steps.

The morphology and layer thickness were studied by planar and cross sectional optical mi-

scopy, while the crystallographic orientation and crystalline quality were determined by four-crystal X-ray diffractometry. Photoluminescence (PL) measurements were performed at 12 K on the buffer layers. Elemental depth profiles were performed on the buffer layers by secondary ion mass spectroscopy (SIMS) in order to determine the abruptness of the substrate/buffer interface. These SIMS measurements were performed using oxygen ion bombardment and positive ion spectrometry was used to measure the concentrations of Ga, As, Cd, Zn and Te. Electrical contact was

made to the buffer layers and I - V measurements performed to determine the resistivity, while Hall measurements were performed between 15 and 300 K on the (CdHg)Te layers.

3. Properties of the buffer layers

3.1. Buffer A: GaAs / CdTe

The growth of CdTe directly onto the desorbed GaAs (100) surface was always found to

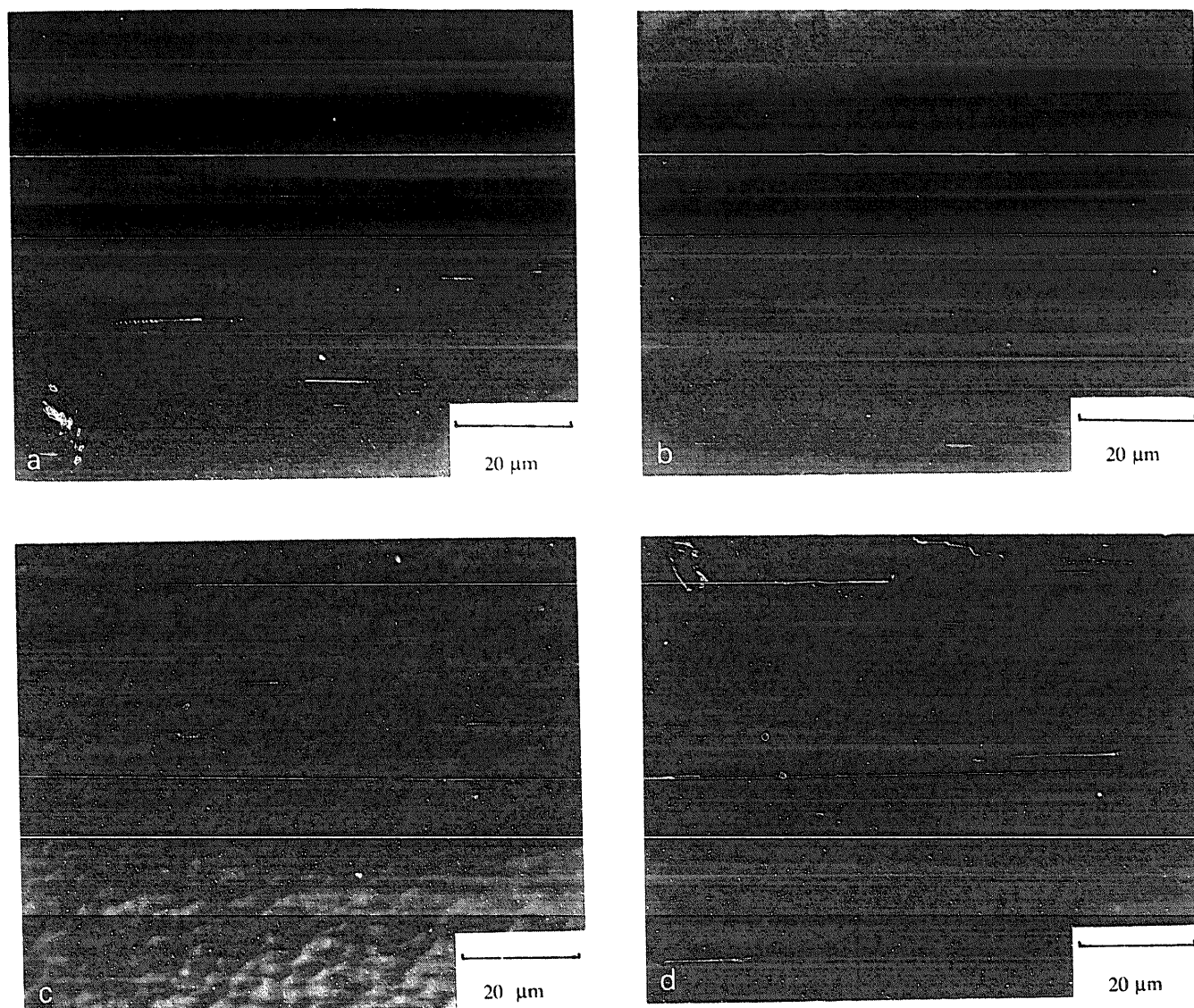


Fig. 2. The surface morphology of the different buffer layers used in this study; (a) buffer A; (b) buffer B; (c) buffer C; (d) buffer D.

lead to the CdTe taking up the (111) orientation. This result is usually ascribed to the fact that the large lattice mismatch can be relieved to some extent when the epitaxial $\langle 110 \rangle$ direction aligns with the substrate $\langle 112 \rangle$ direction, resulting in a low 0.7% mismatch in this direction [5].

The surfaces of these layers appear highly specular to the eye, but when examined under an optical microscope they show a slightly mottled but smooth surface morphology as seen in fig. 2a. Some small hexagonal features (2–3 μm diameter) can be seen under high magnification. When examined by X-ray diffraction these layers show FWHM values for the 333 peak of 350–400 arc sec. The X-ray characterization also indicated

that the layers are twinned. The photoluminescence measurements on these layers tend to show low intensities of luminescence, which may be indicative of the presence of a high density of non-radiative recombination centres. The typical PL spectrum, shown in fig. 3a, shows a small exciton peak at 1.595 eV, together with a large and very broad defect peak centred at 1.47 eV.

3.2. Buffer B: GaAs / ZnTe / CdTe

It has been found that the (111) orientation in (CdHg)Te epilayers leads to the formation of unwanted donor states [3,6]; thus it was attempted to also produce (100) oriented buffer

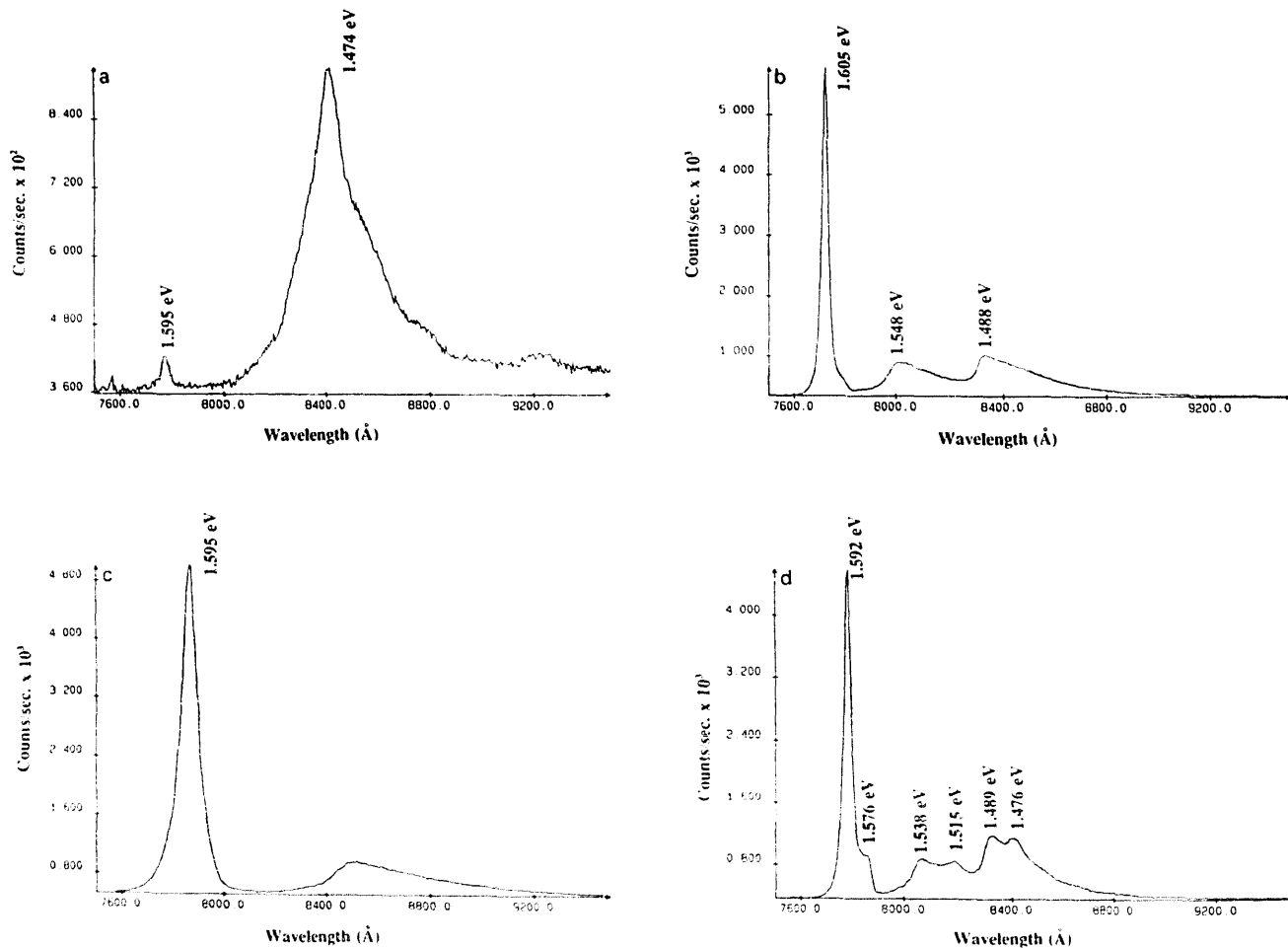


Fig. 3. The 12 K photoluminescence spectra of the different buffer layers; (a) buffer A; (b) buffer B; (c) buffer C; (d) buffer D.

layers. One way to achieve this orientation on (100) GaAs substrates is by means of an intermediate ZnTe buffer [7].

When the ZnTe layers, with a reduced lattice mismatch compared to CdTe, were grown on the desorbed GaAs surface, a parallel epitaxial (100) orientation was obtained. The films again showed a very smooth surface morphology, but with some small surface pyramids visible under the optical microscope. When CdTe buffer layers were deposited on the GaAs/ZnTe combination, these CdTe layers were always found to take up the (100) orientation. The thickness of the intermediate ZnTe layer was found to be critical in determining the quality of the CdTe layers. If a thick ($> 1 \mu\text{m}$) ZnTe layer was used, the CdTe showed a dull appearance with an extremely poor surface morphology. A poor crystalline quality was also indicated by the very large FWHM values of the 400 XRD peak of 1000 to 1200 arc sec. The thickness of the ZnTe layers was progressively decreased by decreasing the growth time of the ZnTe cycle. The thicknesses of those layers that were too thin to be measured in the optical microscope were estimated from the growth rate measured on the thicker layers. It was found that the crystalline structure of the CdTe layer progressively improved as the ZnTe thickness was decreased until a FWHM value of 200–250 arc sec was measured for the CdTe layer at an estimated thickness of 500 Å for the ZnTe (60 s growth time). If the growth time of the ZnTe layer was reduced even more, very inconsistent results were experienced, with the CdTe layer sometimes taking up the (111) orientation or showing a poor (100) crystalline structure. The growth of these buffer layers was then standardized using a ZnTe growth step of 60 s, which would yield an estimated thickness of 500 Å of ZnTe.

These (100) CdTe layers showed the surface pyramids typical of this orientation [8], but by optimizing both growth parameters and the ZnTe thickness, a pyramid density of $< 200 \text{ cm}^{-2}$ could be obtained (fig. 2b). A high PL intensity was obtained and these layers typically showed an intense exciton peak together with some smaller defect peaks, as is shown in fig. 3b. In some of

these layers no discernible defect peaks could be detected above the background.

3.3. Buffer C: GaAs / ZnTe / grading / CdTe

It was attempted to improve the quality of the CdTe buffer layers by grading between the ZnTe and CdTe layers. This grading was done over thicknesses of 0.3 to 0.8 μm and a further 3 μm CdTe was then grown on top of the graded layer. However, these graded layers failed to improve the CdTe quality in any way and the CdTe buffers showed a poorer surface morphology and crystalline quality than the layers with no grading (fig. 2c). The 400 FWHM of these layers varied between 500 to 650 arc sec, while the poor surface morphology is evident in fig. 2c. The PL spectrum, however, still shows an intense exciton peak, while a low but broad defect band can be seen around 1.47 eV in fig. 3c.

A complete range of $(\text{Cd}_x\text{Zn}_{1-x})\text{Te}$ alloys were also grown by varying the Cd:Zn fraction in the vapour phase. The composition of the alloy was determined by X-ray diffraction and photoluminescence. Compositions close to both end points of the alloy were found to produce high quality layers, but the layers deteriorated markedly for intermediate compositions $0.2 \leq x \leq 0.8$. A graph of the variation in FWHM of the 400 X-ray peak as a function of the layer composition is shown in fig. 4. This poor crystalline structure of the intermediate $(\text{CdZn})\text{Te}$ composition may be the rea-

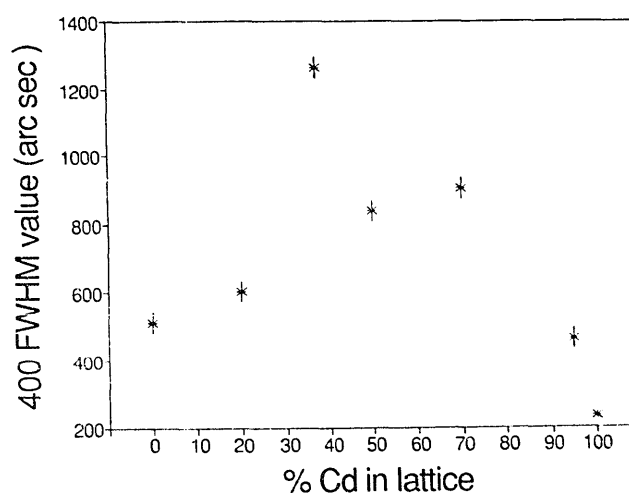


Fig. 4. The FWHM values of the 400 XRD peaks of $(\text{CdZn})\text{Te}$ layers of different composition.

son why these graded layers show such a poor crystalline structure and surface morphology, as the crystal structure would deteriorate when the layer was graded through the intermediate x values of the $(\text{Cd}_x\text{Zn}_{1-x})\text{Te}$ layer.

3.4. Buffer D: $\text{GaAs} / \text{ZnTe} / \text{Cd}_{0.9}\text{Zn}_{0.04}\text{Te}$

A buffer with approximately 4% Zn in the alloy was then grown in order to obtain a close

Table 2
Characteristics of different buffer layer structures

Buffer	Orienta- tion	XRD FWHM (arc sec)	PL ratio	Surface
A	(111)	350–400	< 0.5	Good, small hexagonal features
B	(100)	200–250	3.8	Good, small pyramids
C	(100)	500–650	4.9	Poor, high pyramid density
D	(100)	250–300	5.6	Fair, pyramids

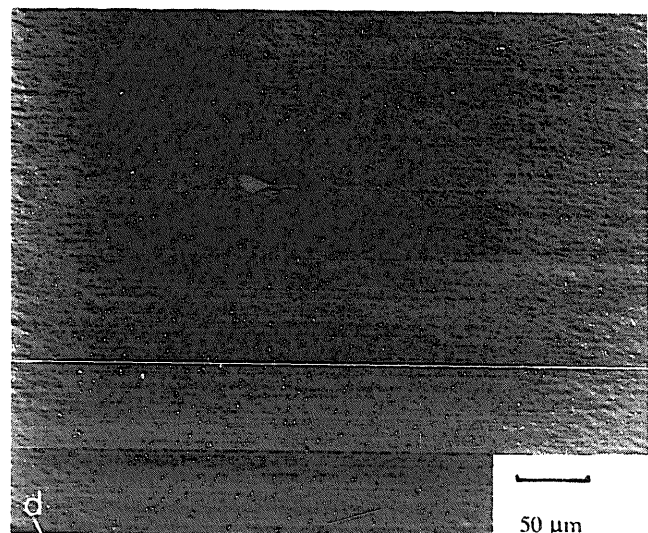
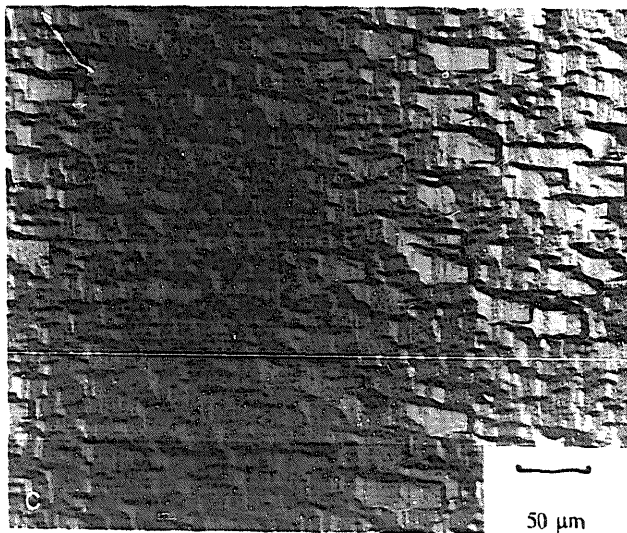
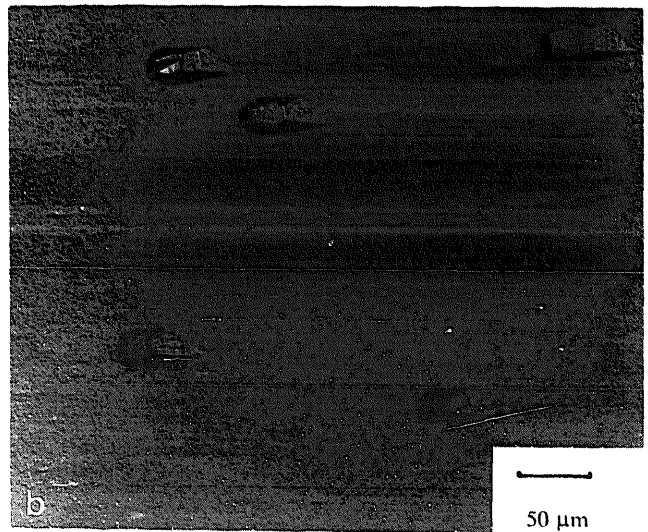
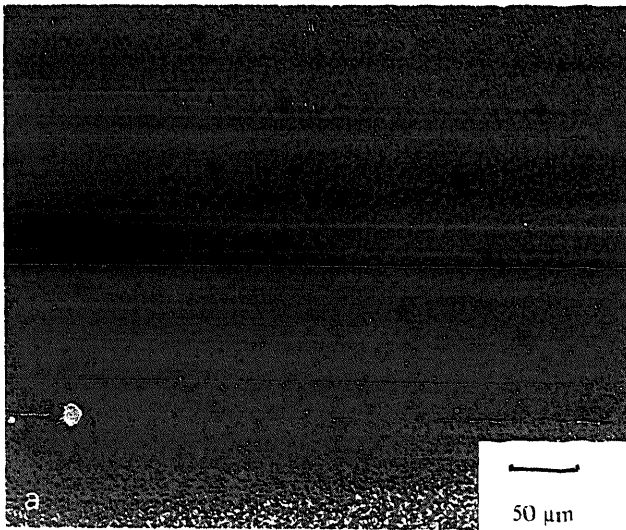


Fig. 5. The surface morphologies of the $(\text{CdHg})\text{Te}$ layers on the different buffer layers; (a) buffer A; (b) buffer B; (c) buffer C; (d) buffer D.

lattice match with $\text{Cd}_{0.2}\text{Hg}_{0.8}\text{Te}$. Although this layer still appears specular to the eye, the surface morphology is slightly deteriorated from that of pure CdTe (fig. 2d). The 400 FWHM shows values of 250–300 arc sec, while the PL spectrum in fig. 3d shows less defect peaks than that of the pure CdTe layer.

Elemental depth profiles were performed by SIMS through all these buffer structures. In all cases the interfaces appeared sharp and very little out-diffusion of Ga could be detected above the detection limit of 10^{16} atoms cm^{-3} . No conclusive evidence could be gained from these different SIMS spectra that a particular buffer structure would be a more effective diffusion barrier than the other. From the I - V measurements all these layers also appeared to be semi-insulating.

In table 2 a summary of the results of the various buffer structures is presented.

4. Characteristics of (CdHg)Te epilayers on the different buffers

4.1. Crystalline perfection

In all cases the (CdHg)Te epilayers were found to take up a similar crystallographic orientation to the buffer layer. The FWHM values obtained from the different layers are shown in table 3. It can be seen that the values obtained on the different buffer layers are fairly close to each other, with the ZnTe/CdTe and the $\text{Cd}_{0.96}\text{Zn}_{0.04}\text{Te}$ producing the best layers and the graded buffers the poorest layers.

4.2. Surface morphology

The surface morphologies of the different (CdHg)Te epilayers obtained on the various buffer layers are shown in fig. 5. The (111) epilayer, obtained on buffer A, show a distinct variation from the other (100) epilayers. Although the surface is slightly dull to the eye, it appears fairly smooth under the microscope and shows only a few large features. The most prominent features are some triangular and hexagonal features of 10–15 μm in diameter. The general background of this film tend to show a somewhat irregular “orange peel” effect.

All three other layers show the typical growth pyramids of the (100) orientation, but show marked variations in the density of these pyramids. The epilayer on buffer C (graded layer) shows the poorest surface, while the epilayer on buffer B (ZnTe/CdTe) shows a marked improvement. However, the quality of the layer on the lattice matched buffer D shows by far the smoothest surface morphology. In table 3 averaged densities of pyramids on the different buffers are indicated.

4.3. Electrical properties – Hall effect

The (111) epilayer grown on buffer A again showed a dramatic variation compared to the other epilayers. From table 3 it can be seen that the other epilayers measured p-type at 77 K, while this (111) layer shows n-type conductivity. This result is often ascribed as being due to the twinning in the (111) structure which leads to donor states with this orientation [3,6].

Table 3
Properties of (CdHg)Te epilayers on different buffers

Buffer	Orienta- tion	XRD FWHM (arc sec)	Pyramid Density (cm^{-2})	Carrier type at 77 K	Carrier concentration at 77 K (cm^{-3})	Carrier mobility at 77 K ($\text{cm}^2/\text{V}\cdot\text{s}$)
A	(111)	110–145	5000	n	2×10^{16}	10000
B	(100)	90–120	4000	p	5×10^{16}	553
C	(100)	170–200	60000	p	6×10^{16}	495
D	(100)	85–110	< 1000	p	5×10^{16}	578

All the (100) epilayers show hole concentrations in the mid 10^{16} cm^{-3} range, as can be expected from thermodynamic considerations, with no significant difference between the various epilayers.

5. Summary and conclusions

The suitability of different buffer layer structures for the growth of (CdHg)Te on GaAs substrates was investigated. These results can be summarized as follows:

(i) If CdTe is deposited directly on the desorbed GaAs surface using the growth conditions described, the (111) orientation always results. This orientation leads to a good surface morphology, but the buffers show a high density of structural defects. Any (CdHg)Te epilayers grown on these buffers also show n-type conduction, most probably due to donor levels resulting from the twinning in the material. This makes this buffer orientation impractical for (CdHg)Te growth.

(ii) The (100) CdTe orientation could be selected by the growth of an intermediate buffer layer of ZnTe. By using the correct thickness of ZnTe, a good quality (100) CdTe layer could be grown.

(iii) Attempts to improve the quality of the buffer layer by grading from ZnTe to CdTe were not successful, probably due to the deterioration of intermediate compositions of the (CdZn)Te alloy. However, good quality $\text{Cd}_{0.96}\text{Zn}_{0.04}\text{Te}$ was grown as a lattice matched buffer.

(iv) All the (100) (CdHg)Te epilayers showed p-type conductivity as expected from thermodynamic considerations with a mid 10^{16} cm^{-3} hole concentration. However, the surface morphology of the different layers shows a strong variation, with the graded layer producing the poorest surface and the $\text{Cd}_{0.96}\text{Zn}_{0.04}\text{Te}$ buffer the best surface morphology. It is possible that this improvement in morphology is due to the better lattice

matching between substrate and epilayer. Similar results have been found in the growth of (CdHg)Te on CdTe compared to lattice matched CdTeSe and CdZnTe substrates [9,10].

(v) It is thus concluded that of the buffer layer structures evaluated, the lattice matched (CdZn)Te alloy shows much promise for (CdHg)Te epitaxy. It would seem able to improve the surface morphology of the (100) epilayers compared to the non-lattice-matched CdTe buffers, while the electrical properties of the layer appears unaffected by the different buffer structure. Despite this improvement in surface morphology in the lattice matched structure, the surface pyramids could never be eliminated completely.

(vi) At present, good quality (CdHg)Te epilayers are routinely grown on 50 mm diameter GaAs substrates using buffer B (ZnTe/CdTe). Uniformity problems are still experienced in producing lattice matched (CdZn)Te buffers of the correct composition over these large areas, so that no (CdHg)Te growth has yet been attempted on 50 mm substrates using buffer D.

References

- [1] I.L. Schmidt, *J. Vacuum Sci. Technol.* A 4 (1986) 2141.
- [2] S.J.C. Irvine, J.B. Mullin, J. Giess, J.S. Gough, A. Royle and G. Grimes, *J. Crystal Growth* 93 (1988) 732.
- [3] L.M. Smith, C.F. Byrne, D. Patei, P. Knowles, J. Thompson, G.J. Jenkin, T. Nguyen Duy, A. Durand and M. Bourdillot, *J. Vacuum Sci. Technol.* A 8 (1990) 1078.
- [4] J. Tunnicliffe, S.J.C. Irvine, O.D. Dosser and J.B. Mullin, *J. Crystal Growth* 68 (1984) 245.
- [5] H. Booyens and J.H. Basson, *South African J. Sci.* 84 (1988) 705.
- [6] R. Triboulet, *J. Crystal Growth* 107 (1991) 598.
- [7] R.D. Feldman, R.F. Austin, A.H. Dayem and E.H. Westerman, *Appl. Phys. Letters* 49 (1986) 797.
- [8] P. Capper, C.D. Maxey, P.A.C. Whiffen and B.C. Easton, *J. Crystal Growth* 96 (1989) 519.
- [9] I.B. Bhat, H. Fardi and S.K. Ghandhi, *Appl. Phys. Letters* 52 (1988) 392.
- [10] M.J. Bevan, J. Greggi and N.J. Doyle, *J. Mater. Res.* 5 (1990).